Design and modeling of an electrochemical device producing methane/oxygen and polyethylene from in-situ resources on Mars

Final Report to Opus 12, Inc.

Dr. Jeffery B. Greenblatt
Emerging Futures, LLC

Submitted October 3, 2018
Updated for public release: June 7, 2019

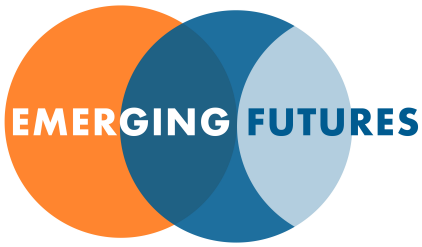

Jeffery B. Greenblatt, Ph.D.
Founder, CEO and Chief Scientist
Emerging Futures, LLC
2726 Eighth St.
Berkeley, CA 94710

jeff@emerging-futures.com
+1.510.693.6452
@EmergingFutLLC
EmergingFutures.space
Imagining Tomorrow's Sustainable Technologies Today™

Design and modeling of an electrochemical device producing methane/oxygen and polyethylene from in-situ resources on Mars

Final Report

Dr. Jeffery B. Greenblatt
Emerging Futures, LLC

October 3, 2018

Project summary

Opus 12 is developing a technology that will enable the one-pot synthesis of methane (CH_4) and/or ethylene (C_2H_4) from Martian CO_2 and water using electricity. Oxygen (O_2) is the other major product. Minor reduced products such as H_2, CO, etc. are also synthesized and must be separated. CH_4 and/or C_2H_4 can be used along with O_2 as a propellant for spacecraft or surface applications. C_2H_4 can also be fed into a secondary reactor to make common plastics such as polyethylene. It was assumed that existing equipment on the surface of Mars would supply pure CO_2, H_2O and electricity as inputs to our device.

Emerging Futures, LLC, as a subcontractor to Opus 12, has been tasked with performing system analysis and design of a thermal management system, identification of uses of rejected heat for separations, and design of a full CO_2-to-plastic reactor.

Part I: CO_2-to-propellant device design

The first part of the project was to develop the balance-of-system components needed to convert the raw output from the Opus 12 electrochemical (EC) cell into usable products, e.g., propellant (fuel + oxygen). The EC cell produces a variety of reduced products at the cathode, including methane (CH_4), ethylene (C_2H_4), hydrogen (H_2), carbon monoxide (CO), ethanol (C_2H_5OH) and small amounts of other light (C_1-C_3) hydrocarbons such as formate, acetaldehyde, etc.[1] The initial approach was intended to produce nearly-pure CH_4 as the primary fuel, but our research revealed that it is quite difficult technically to separate CH_4 and C_2H_4, so our design centered on producing a well-defined mixture of CH_4 and C_2H_4 that could be used with O_2 as a rocket propellant, with nearly the same specific impulse (I_{sp}) as $CH_4 + O_2$, around 360 s. (See Appendix section 1 for more details.)

Figure 1 shows the major components of the CO_2-to-propellant device, consisting of a pressurization pump, EC cell, water-gas shift (WGS) reactor (including heater, reactor stages and heat exchangers), gas dryers to remove H_2O, membrane separators, and heat radiators. Of note is

[1] For modeling purposes, we assumed a representative snapshot product distribution of 50% CH_4, 30% C_2H_4, 3% H_2, 3% CO and 14% ethanol by energy, or 51.6%, 19.6%, 9.6%, 9.7% and 9.4% respectively by volume. The device was subsequently able to achieve >50% CH_4 or C_2H_4 depending on catalyst and reaction conditions.

the WGS reactor, which converts CO + H_2O into H_2 + CO_2. CO is difficult to separate using membrane techniques, but relatively straightforward to convert to H_2 thermochemically, and H_2 is much easier to separate from other gases. Since CO_2 and H_2 are already present in the product mixture and must be separated, an increase in the quantities of these gases does not add any significant complexity to the overall design. (Details of the WGS system can be found in the Appendix section 2.)

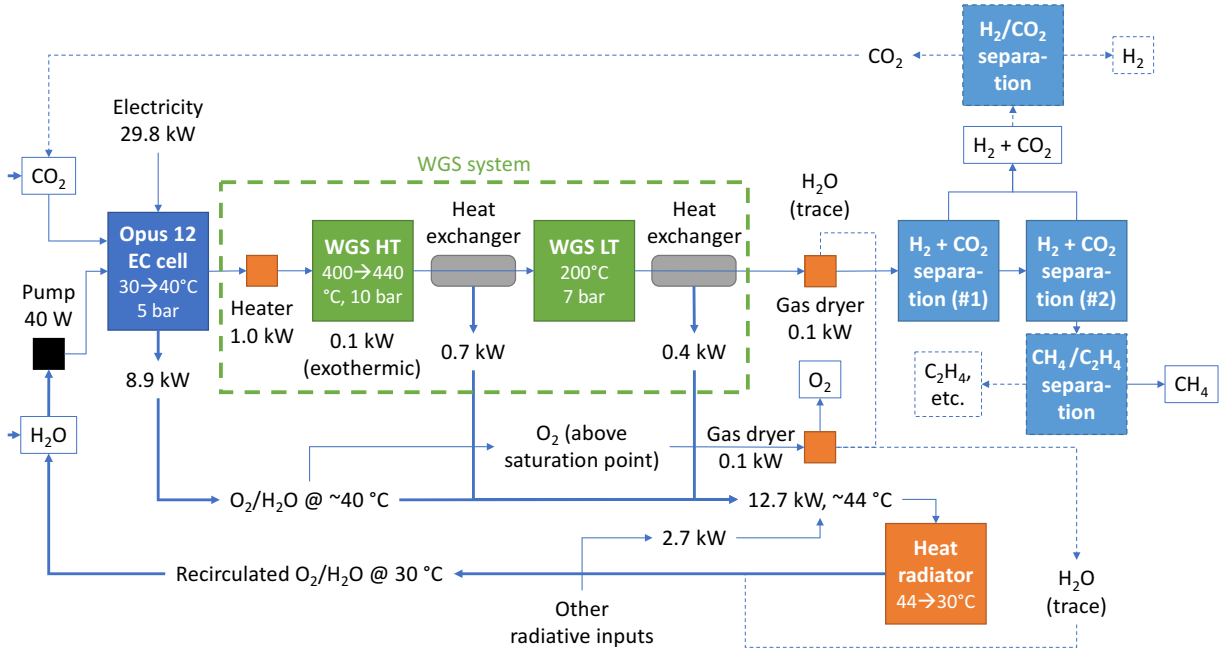

Figure 1. Major components of the CO_2-to-propellanrt reactor design

Note that the gas dryers are cycled periodically (about once per hour) to liberate captured H_2O; the resulting ~2.5 kg/d can be either reinjected into the cell, or discarded. The physical design layout of the WGS subsystem is given in Figure 2.

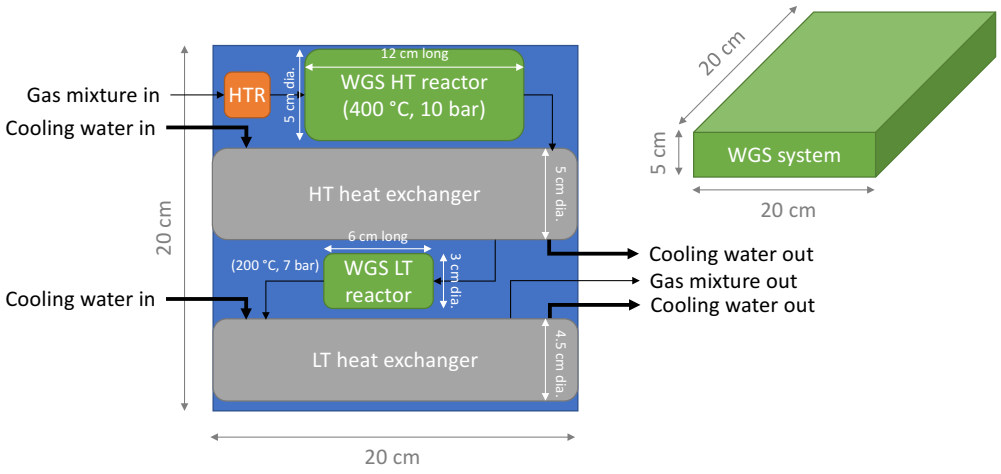

Figure 2. Water gas shift design layout

Approaches for removing H_2O from product gases (fuel mixture and O_2) are discussed in the Appendix section 3. The separation of gases is assumed to take place in at least two stages. MTR Inc. developed a membrane-based separator design for us that simultaneously removes H_2 and CO_2, leaving most of the CH_4 and C_2H_4 intact (Tim Merkel, pers. commun., 2017; see details in the Appendix section 4). A single-stage configuration removes approximately 25% of the CH_4 and C_2H_4, whereas a two-stage configuration, requiring two compression steps, removes only 10%. We opt for the two-stage configuration due to its much lower loss rate. We assume, based on parameters supplied by MTR, that each stage requires ~1 m^2 of membrane area and occupies a cylinder volume of 20 cm in diameter and 2.2 cm in height.

H_2 and CO_2 can be subsequently separated with high efficiency using a standard membrane. Room for additional separation stages (e.g., H_2 from CO_2, or CH_4 from C_2H_4) with up to ~4 m^2 of membrane area is feasible, and is included as a contingency. These extra stage(s) would in total occupy a cylinder 20 cm in diameter and 9 cm in height. Each stage would be driven by a compact scroll-type compressor 20 cm diameter whose total height for three compression stages is ~26 cm.

Figure 3 shows the device integrated into a complete system that includes regolith and atmospheric extraction processes. The elements inside the red box are unique to the Opus 12 system, whereas elements outside it are also present in a conventional Sabatier reactor-based design. (See Appendix section 5 for more information.) However, because gas separation is intrinsic to producing the desired products, we include these separation steps in our Opus 12 design along with the other components inside the red box.

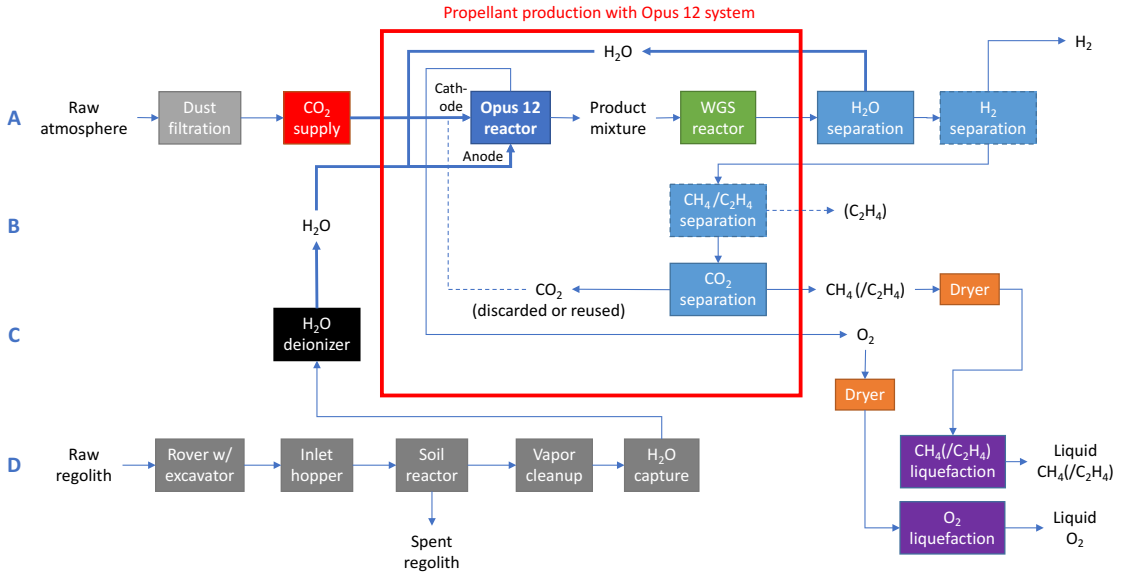

Figure 3. Diagram of CO_2-to-propellant overall device design

The physical system layout, including the large heat radiators that are required to reject the waste heat generated by the system, is shown in Figure 4. The fully-stowed device including radiator panels is 66 cm long, 66 cm wide, and 60 cm high. There are four symmetrically folded panels against the sides of the central "device core" containing a water pump, EC cells, WGS reactor, gas dryers, and multiple separation stages. The fully-extended radiator panel area is 26.9 m^2

(double-sided), configured as four panels each measuring 5.59 m long (folded into 13 segments each 43 cm long) by 60 cm high. Heat is removed from the EC and WGS reactors using water circulated through the anode side of the device. The fuel gas stream is dried prior to separation, and the O_2 gas stream is separated from the water and dried just prior to use. The H_2O stream sent to the radiator panels remains saturated in O_2 (about 0.65 mass% at 40 °C), but proper coating of materials should prevent any degradation. Schedule 5 aluminum pipe is used for the radiator panel tubing, as it is the least massive yet has a maximum burst pressure of ~400 bar (Engineering Toolbox, no date; aluminum has a burst pressure ~50% that of stainless steel; TubeWeb, no date), many times higher than the expected maximum pressure of 10 bar. An outer diameter of 1.72 cm (3/8 inch nominal pipe size) was chosen to keep the total pressure drop in each panel at ~0.5 bar including bends. The total pipe length is 1.57 km (sum of all panels).

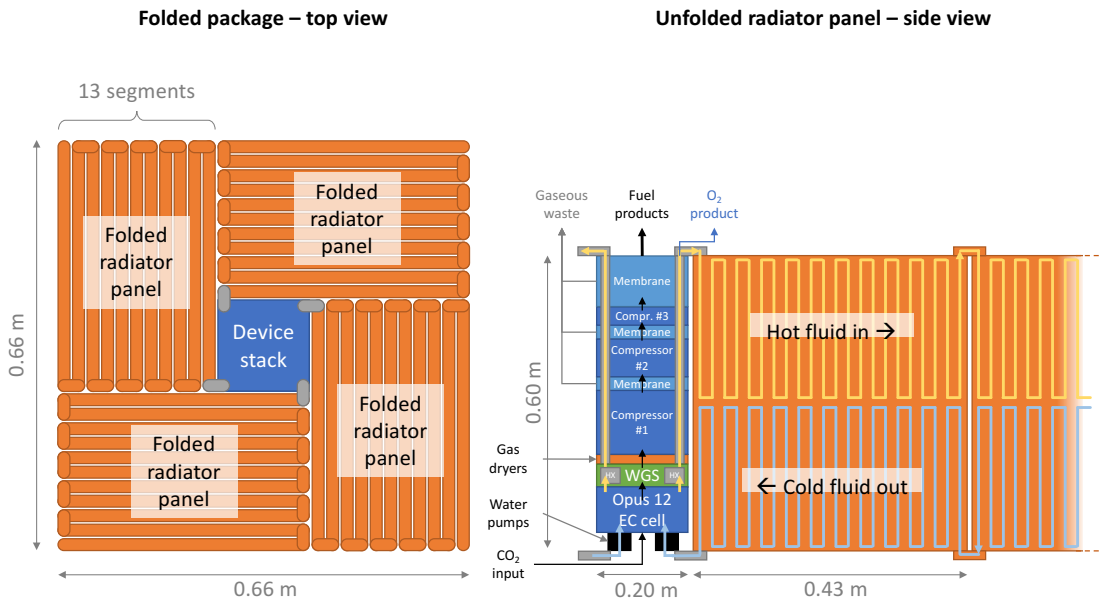

Figure 4. Overall device physical layout.

A mass breakdown of the complete system is summarized in Table 1.

Table 1. Mass breakdown of CO_2-to-propellent system

Component	Mass (kg)	Component	Mass (kg)
Water pump	0.9	Gas dryers	3.0
EC stack	124.0	Gas compressors	11.6
WGS reactors	1.1	Membrane separation stages	5.9
Heat exchangers	0.3	Radiator panels	264.9
WGS heater	0.5	Total	412.2

Note that this design produces the target CH_4 output rate of 14.6 kg/day or 7.03 t after 480 days (plus sufficient O_2) to resupply propellant to the NASA Design Reference Architecture 5.0 (DRA 5.0) Mars Ascent Vehicle (Kleinhenz and Paz, 2017). It also produces 9.7 kg/day C_2H_4, 0.77 kg/day H_2 and 66.85 kg/day additional O_2. If a CH_4/C_2H_4 mixture were used instead, the mass could in principle be reduced to 249 kg while still providing sufficient propellant.

We have explored the sensitivity of the system mass to several key parameters; see Appendix section 6 for details.

Part II: CO_2-to-plastics reactor design

The second part of the project was to develop a design to convert the C_2H_4 produced in the Opus 12 EC cell into high-density polyethylene (HDPE), a common and versatile plastic that can be used to fabricate many useful objects including containers, tools, furniture, etc. as well as high-quality radiation protection. HDPE requires far milder pressures (10-80 atm) than low-density polyethylene (LDPE), which requires >1,000 atm. Reaction temperatures for making HDPE are also modest (80-150 °C),[2] and the polymer is produced below its melting point.

Figure 5 shows the major components of our CO_2-to-plastics reactor design. While outside the scope of our design, the resulting HDPE product would likely be stored as small granules in bags, or perhaps formed into solid blocks to avoid the need for containers. To make a desired material, the polymer could be re-melted before being cast or extruded, or ground into a fine powder prior to 3D printing.

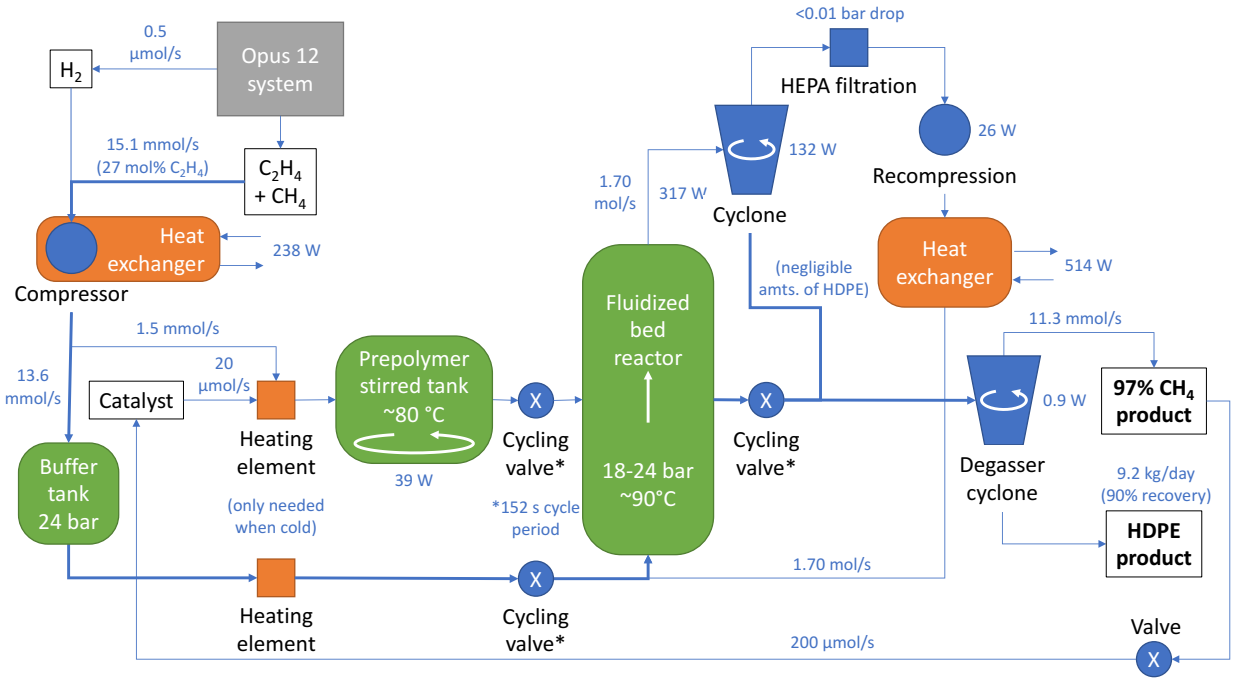

Figure 5. Diagram of CO_2-to-plastics reaction design

We assume that the Opus 12 PEC cell produces a mixture of C_2H_4 and CH_4; the latter species does not participate in the polymerization reaction and so can be tolerated even if it constitutes >50% of the gas volume. Small amounts of CO_2 may also be present, but as this gas also does

[2] Note that both CH_4 and C_2H_4 become supercritical at temperatures well below this range above ~50 bar. The impact of potentially supercritical CH_4 on the C_2H_4 polymerization process is unclear, but should be investigated in follow-on work.

not react with other chemical species under the conditions of the polymer reactor, it is considered (along with CH_4) to be an inert buffer gas. The reactor also requires a small amount of H_2 (0.01 mol% of C_2H_4) which acts to terminate the polymerization reaction, as well as a polymerization catalyst (0.5 mol% of C_2H_4). For details, see the Appendix section 7.

The resulting polymer product removes nearly all the C_2H_4 from the input gas stream, resulting in a final gas mixture that is 97% CH_4. A small portion (~2%) is used as an inert buffer gas to entrain catalyst particles into the reactor; the rest can be used as a nearly-pure CH_4 product, potentially for use as propellant in a rocket engine.

The additional heat load that must be removed from the CO_2-to-plastics reactor is modest, about 750 W (see Appendix section 7 for details). If integrated with the same heat radiator system as described earlier, the radiator area would increase 7% to 28.7 m^2, add an additional 19 kg to the system mass, and increase the device footprint to 72 cm by 72 cm.

The mass budget for the CO_2-to-plastic reactor is summarized below in Table 2. The total mass of this system (17 kg) plus the additional required radiator panel mass (19 kg) is less than 10% of the mass of the CO_2-to-propellant system (412 kg). While also easily fabricated on Earth, the tremendous mass leverage afforded by making HDPE on Mars (producing its own mass in HDPE in 3.7 days) can provide valuable cost savings and design flexibility. Therefore, for a small increment in total mass, the system could be enhanced to provide not only ~9 kg/day of high-quality HDPE plastic, but also >95% CH_4 for use as rocket propellant.

Table 2. Mass budget of CO_2-to-plastics system

Component	Mass (kg)	Component	Mass (kg)
Initial compressor	1.88	HEPA filter	1.64
Prepolymer tank	0.30	Precompression heat exchanger	0.84
Buffer tank	1.93	Main heat exchanger	0.84
FB reactor	2.35	Recompressor	0.21
Cyclone	7.03	Degasser	0.05
		Total	17.06

Conclusions and future directions

We have developed a preliminary device design that can produce from CO_2 and H_2O from Martian resources 14.6 kg/day of CH_4 and 58.6 kg/day of O_2, sufficient to refuel a NASA DRA5.0 Mars Ascent Vehicle in 480 days. In fact, there is 66.6 kg/day of O_2 left over for other purposes. The device also produces 9.7 kg/day of C_2H_4 that can either be converted into HDPE plastic in a separate reactor, or mixed with CH_4 to provide 66% more rocket propellant with almost no change in I_{sp}. In addition, the device produces 0.77 kg/day of H_2. The overall mass of the combined propellant + plastic product system is 449 kg.

There is a possibility of using the Martian atmosphere for convective cooling similar to forced-air cooling on Earth; other related devices (e.g., a Mars nuclear reactor; Morrison, 2018) have successfully incorporated this concept into their design. Based on conversation with their designer, we estimate that such an approach would require an additional ~1.3 kW of power but

may shrink the radiator cooling area significantly. Additional work is needed to fully validate this approach.

Appendices

1. $CH_4/C_2H_4 + O_2$ I_{sp} calculations

We utilized a NASA model to calculate the specific impulse (I_{sp}) of combustion of various mixtures of CH_4 and C_2H_4 with different fuel:O_2 ratios, assuming 1000 psi and 93% combustion efficiency. Gerald Sanders (NASA Johnson) provided these results in a private communication in September 2016, which are summarized in Table 3:

Table 3. Calculated vacuum specific impulse (I_{sp}) for various CH_4/C_2H_4 and fuel:O_2 mass ratios.

Fuel:O_2 mass ratio	**100 wt% CH_4**	**90 wt% CH_4 10 wt% C_2H_4**	**75 wt% CH_4 25 wt% C_2H_4**	**57 wt% CH_4 43 wt% C_2H_4**
	I_{sp} (s)			
2.0	316.89	319.96	324.63	330.29
2.5	338.99	341.50	345.10	349.10
3.0	352.31	353.80	355.74	357.53
3.5	357.47	357.70	357.56	356.44
4.0	353.56	352.31	350.31	347.78

Assumptions: 1000 psi, 93% combustion efficiency. Source: Gerald Sanders, NASA Johnson.

For a 3.5 fuel:O_2 mass ratio that maximizes the I_{sp} for pure CH_4, we found almost no difference (<0.1%) in I_{sp} between a 100% CH_4 and 90 wt% CH_4/10 wt% C_2H_4 mixture. Even for a 57 wt% CH_4/43 wt% C_2H_4 mixture, the difference in I_{sp} was <0.3%. Therefore, there is no real performance impact of using CH_4/C_2H_4 mixtures. In fact, for lower fuel:O_2 mass ratios, the addition of C_2H_4 appears to improve the I_{sp}; for instance, for a fuel:O_2 mass ratio of 3.0, the highest I_{sp} is achieved with a 57 wt% CH_4/43 wt% C_2H_4 mixture.

2. WGS system

The WGS reaction proceeds more rapidly at higher temperatures, but products are thermodynamically more favored at lower temperatures (Lima et al., 2012; Wikipedia, 2017). Therefore, industrial-scale reactions are generally designed in two steps, starting with a high temperature (HT) reaction (at ~400 °C) which converts ~80% of the CO into CO_2 (and H_2O into H_2), followed by a lower temperature (LT) reaction (at ~200 °C) to remove all but ~0.1% of the CO. Pressures range from ~1 bar up to ~80 bar; in the system we modeled, 10 bar was assumed, following Ma et al. (2009). If the CO concentration is sufficiently low (less than ~2-4%), it may be possible to only employ the LT reactor; however, more research would be required to determine ideal reaction conditions for such a system. In our system, 5 mol% CO is assumed in the overall raw product gas stream.

A typical HT catalyst is "ferrochrome" (74-95% Fe_2O_3 or Fe_3O_4 + 5-10% Cr_2O_3, with small amounts of Cu or other oxides, e.g., K, Mg, Zn, Pb, Al), whereas typical LT catalysts are

Cu/Zn/Al or Cu/Ce/La oxides (Callaghan, 2006; Ma et al., 2009; Lima et al., 2012, Wikipedia, 2017). Scaling down from an industrial-sized design (Ma et al., 2009) handling 1,500 mol/s CO to ~2.3 mmol/s implied by our parameter assumptions (total product flow rate of 24 mmol/s and ~10 mol% CO), we calculate required dimensions of a 3.8 cm (inner diameter) by 11 cm (length) cylinder for the HT reactor, and a 2.7 cm (inner diameter) by 7 cm (length) cylinder for the LT reactor. Ma et al. assumed catalyst densities of ~1 g/cm^3 for both reactors, implying available volumes of ~80% of total (empty) cylinder volumes. With assumed temperatures of 400 and 200 °C, and pressures of 10 and 7 bar, we calculate residence times of 7.9 and 2.6 s in the HT and LT reactors, respectively.

To manage the temperature changes of the WGS reactor, we include an electric resistance heater to raise the temperature of the raw product gas mixture from ~40 °C to 400 °C (see Figure 1). The mass of this heating unit was estimated to be ~0.5 kg, based on compact metal-ceramic heaters (Thorlabs, 2018) also used in the gas dryer design. Using the estimated enthalpies for this temperature change of each gas in the mixture (including the vaporization of H_2O), the required energy is ~990 W. Because the reaction is exothermic, an additional ~100 W are generated by the reaction, with ~80 W in the HT reactor and ~20 W in the LT reactor. Therefore, a total of ~1.1 kW must be removed from the system to return it to 40 °C. This is accomplished by circulating H_2O from the anode side of the EC reactor through both the HT and LT reactors with sufficient contact areas to lower the temperatures by the desired amounts. Two heat exchangers are included to remove the heat after each reactor stage, whose dimensions are based on necessary contact areas and an assumed overall system heat coefficient of 200 W/m^2-K.

At these elevated temperatures, we needed to ensure that the maximum pressure ratings would not be exceeded. Note that the additional heat provided by the exothermic reaction raises the HT reactor temperature to ~450 °C. For the HT reactor at this temperature, our assumed 1.5-inch Schedule 80 stainless steel pipe has a maximum pressure rating of 21.6 bar. For the LT reactor at 200 °C, our assumed 1-inch Schedule 40 stainless steel pipe has a maximum pressure rating of 25.9 bar. Because of concern over the use of stainless steel in contact with H_2, we opt for carbon steel, whose maximum rated pressures are 80% that of stainless steel (TubeWeb, no date). The resulting modified pressure ratings still exceed the expected maximum 10 bar pressure by more than 70%.

3. Moisture removal from product gas streams

The natural gas industry employs at least two methods of removing residual water vapor from gases (Hoskins, 2017). The first method involves lowering the gas temperature to cause the water to condense into a liquid or solid, whereas the second method passes the gas mixture through a desiccant that absorbs the moisture; the material is then recharged through heating, driving off the water vapor. Solid desiccants include silica gel, molecular sieves, activated alumina or activated carbon, whereas the preferred liquid desiccant is triethylene glycol.

Both methods require cycling to liberate the captured H_2O. The advantage of the first method is that it does not require a specialized material that could degrade over time; moreover, on Mars it is straightforward to achieve the required temperatures to condense water simply by passing the

gas loop outside of the device into the ambient cold atmosphere. However, such a system is cumbersome, requiring additional piping and heat exchange contact area with the atmosphere.

The second method, while not without drawbacks, has the advantage of being relatively compact, and many desiccants can be regenerated at temperatures of 175-315 °C. It is estimated that such systems require an energy input of ~6.0 MJ per kg of H_2O removed, assuming 70% heating efficiency (Sigma-Aldrich, 2017). These desiccants are not known to degrade, so can be used for many years of service.

While either method will work in principle, we have opted for the latter approach, utilizing a molecular sieve desiccant such as Type 3A (0.6 K_2O : 0.4 Na_2O : 1 Al_2O_3 : 2 SiO_2) from Sigma-Aldrich. This material, with a dry bulk density of 720 kg/m^3, can absorb ~20% H_2O by weight and is regenerated at a temperature between 175 and 260 °C. We have estimated the following H_2O flow rates and required desiccant parameters for the fuel and O_2 sides of the system. The H_2O content of each gas stream was calculated as follows. For fuel, we make a conservative estimate of the remaining H_2O after the WGS reaction. For O_2, we use the vapor pressure of H_2O at 40 °C (0.073 bar) compared with the pressurized O_2 gas stream (5 bar). See Table 4.

Table 4. Desiccant requirements to remove moisture from fuel and O_2 gas streams

Parameter	**Fuel**	**O_2**	**Total**	**Units**
Gas flow rate	1.71×10^{-3}	1.45×10^{-3}		kg/s
H_2O content	1.0%	0.8%		% mass
H_2O flow rate	1.71×10^{-5}	1.22×10^{-5}	2.93×10^{-5}	kg/s
	1.47	1.06	2.53	kg/d
Required desiccant (24 h cycle time)	7.4	5.3	12.7	kg
Required desiccant (1 h cycle time)	0.31	0.22	0.53	kg
Required power (average)	102	73	176	W
1-h cycle time design:				
Required power (2.4 min. peak)	2,558	1,835	4,394	W
Desiccant volume	4.26×10^{-4}	3.06×10^{-4}	7.32×10^{-4}	m^3
Heating element volume	7.25×10^{-5}	5.20×10^{-5}	1.25×10^{-4}	m^3
Total volume	4.99×10^{-4}	3.58×10^{-4}	8.57×10^{-4}	m^3
Desiccant mass	0.31	0.22	0.53	kg
Heating element mass	1.45	1.04	2.49	kg
Total mass	1.76	1.26	3.02	kg
Dimensions:				
Length	0.200	0.200	0.200	m
Width	0.116	0.084	0.200	m
Height	0.021	0.021	0.021	m

An hourly recharge cycle will greatly reduce the mass of desiccant required, so we opt for this configuration in our design. Approximately 0.5 kg of material is needed in total. In addition, the design requires heaters to liberate the H_2O during an hourly recharge cycle lasting 2.4 min., resulting in 96% uptime. Due to the short cycling time, the peak power draw of the heaters is sizable, about 4,400 W. We have identified a commercially-available, flat metal-ceramic heater

that provides the required energy input across the desiccant area when arranged in a double-layer (top and bottom) configuration, with a maximum ambient temperature of 400 °C (Thorlabs, 2018). The heating elements add 2.5 kg, bringing the total mass of the moisture removal system to 3.0 kg. We estimate the combined physical dimensions of the two dryers to be 20 cm by 20 cm by 2.1 cm, and are arranged side-by-side with the fuel dryer occupying 11.6 cm width and the O_2 dryer the remaining 8.4 cm width. See Figure 6.

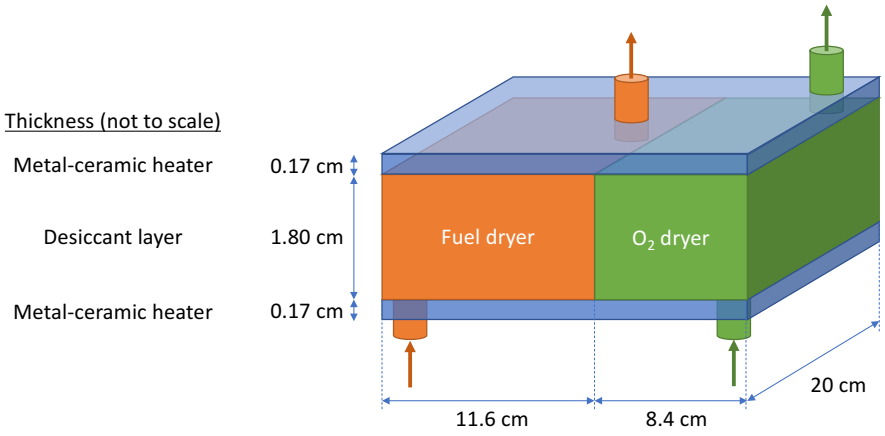

Figure 6. Gas dryer design

4. MTR Inc. H_2 + CO_2 membrane separation subsystem

MTR, Inc. provided Emerging Futures with calculations of a preliminary membrane separation of CH_4 + C_2H_4 from other product gases, assuming CO was first shifted to H_2 + CO_2 via the WGS reactor (Tim Merkel, pers. commun., 2017). See Figure 7.

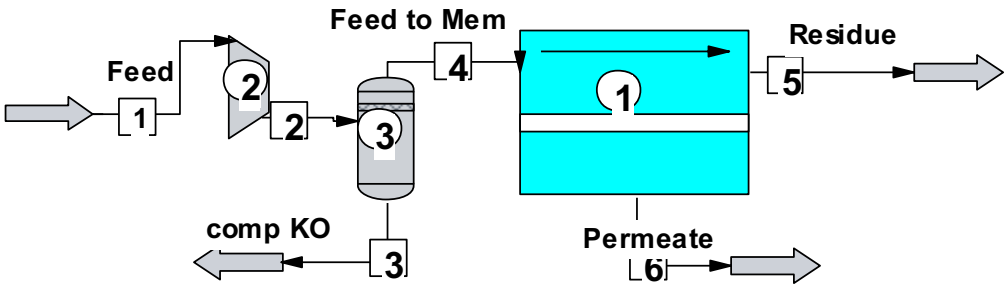

Stream No.	1	2	3	4	5	6
Name	Feed	Comp out	comp KO	Feed to Mem	Residue	Permeate
- - Overall - -						
Molar flow kmol/h	0.0426	0.0426	0.0049	0.0377	0.0111	0.0266
Mass flow kg/h	1.3750	1.3750	0.1495	1.2255	0.2316	0.9939
Temp C	40.0000	300.4230	30.0000	30.0000	-2.1181	13.9410
Pres bar	1.0135	10.0000	10.0000	10.0000	9.9000	1.0000
Std vap 0 C liter/min	15.9225	15.9225	1.8273	14.0952	4.1642	9.9310
Component mole %						
Hydrogen	4.744711	4.744711	0.000665	5.359728	0.681161	7.321531
Methane	23.723602	23.723604	0.005966	26.798350	64.673567	10.916618
Carbon Monoxide	0.000000	0.000000	0.000000	0.000000	0.000000	0.000000
Carbon Dioxide	50.730604	50.730604	7.823285	56.293094	3.727220	78.334868
Ethylene	9.489463	9.489463	0.007623	10.718687	30.516148	2.417268
Ethyl Alcohol	4.744711	4.744711	37.473643	0.501746	0.399936	0.544437
Water	6.566910	6.566911	54.688823	0.328406	0.002003	0.465272

Stream No.	1	2	3	4	5	6
Name	Feed	Comp out	comp KO	Feed to Mem	Residue	Permeate
Flow rates in kg/h						
Hydrogen	0.0041	0.0041	0.0000	0.0041	0.0002	0.0039
Methane	0.1622	0.1622	0.0000	0.1622	0.1157	0.0466
Carbon Monoxide	0.0000	0.0000	0.0000	0.0000	0.0000	0.0000
Carbon Dioxide	0.9516	0.9516	0.0168	0.9348	0.0183	0.9165
Ethylene	0.1135	0.1135	0.0000	0.1135	0.0954	0.0180
Ethyl Alcohol	0.0932	0.0932	0.0844	0.0087	0.0021	0.0067
Water	0.0504	0.0504	0.0482	0.0022	0.0000	0.0022

Figure 7. Design of product gas separation provided by Tim Merkel (MTR, Inc.)

The design separates nearly 100% of H_2, CO_2, ethanol and water, but did not focus on separation of CH_4 from C_2H_4. The figure summarizes the design, which included a compression stage that also removed 91% of the ethanol and 96% of the water prior to membrane separation. Starting from an initial gas mixture of 50.7 mol% CO_2, 23.7 mol% CH_4 and 9.5 mol% C_2H_4, the resulting product stream contained 64.7 mol% CH_4 and 30.5 mol% C_2H_4, with most of the remaining gas being CO_2 (3.7%). The total membrane area required for our assumed 14.6 kg/day CH_4 flow rate (about 3.8 times the modeled flow) was ~1.9 m^2; see Figure 8. However, about 25% of the CH_4/C_2H_4 mixture is lost in the permeate stream; MTR indicated that a two-stage separation design could reduce loss to ~10%.

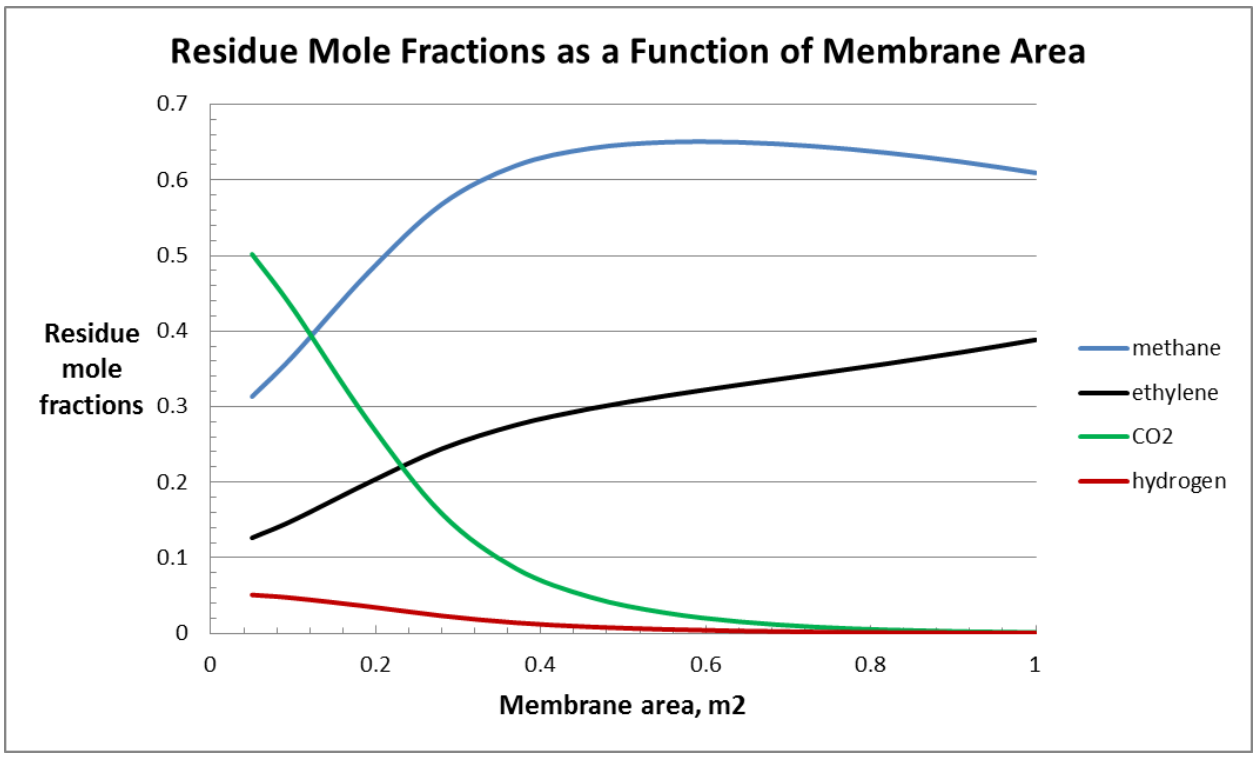

Figure 8. Effect of membrane area on residue mole fractions

5. Sabatier reactor

Kleinhenz and Paz (2017) developed a schematic overview of a $CH_4 + O_2$ production device using Martian resources based on the Sabatier reaction. See Figure 9:

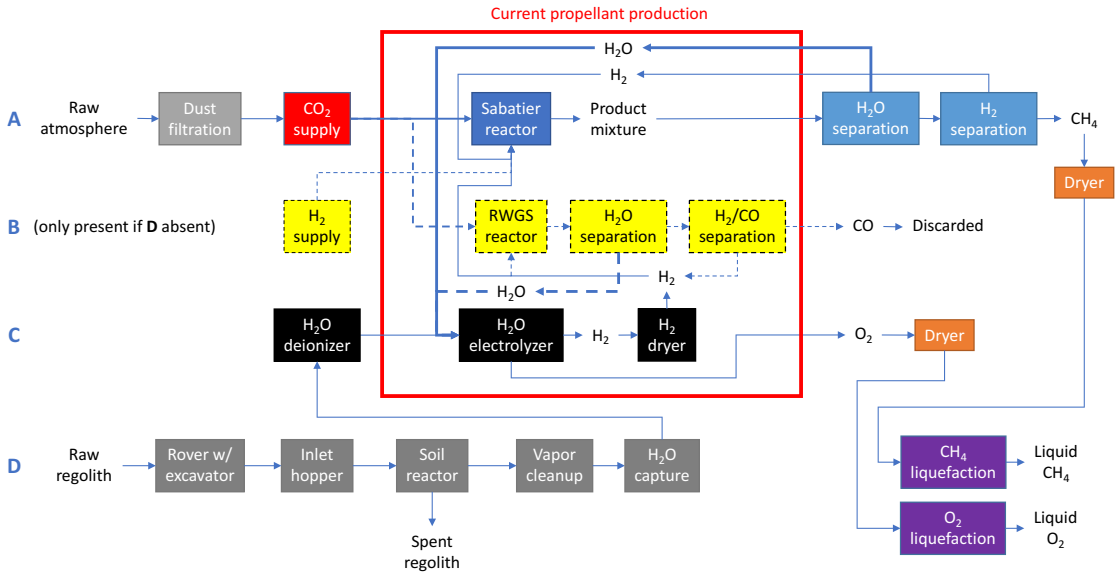

Figure 9. Diagram of conventional Sabatier approach elements

Figure 9 represents two possible configurations:

1. Using both Martian CO_2 and H_2O (from regolith), the electrolyzer produces all the H_2 needed as an input to the Sabatier reactor, plus all the O_2 required for a stoichiometric CH_4:O_2 (1:2 mole) ratio. The chemical reactions involved are:

   Electrolysis: $4H_2O \rightarrow 4H_2 + 2O_2$
   Sabatier: $CO_2 + 4H_2 \rightarrow CH_4 + 2H_2O$
   Net: $CO_2 + 2H_2O \rightarrow CH_4 + 2O_2$ (stoichiometric ratio)

2. Using only Martian CO_2, the H_2 must be supplied from Earth; about 1,750 kg would be required to meet the DRA5.0 CH_4 production target. In this case, a reverse water-gas shift (RWGS) reactor is also needed to produce sufficient O_2 to meet the stoichiometric ratio. The chemical reactions are:

   Sabatier: $CO_2 + 4H_2 \rightarrow CH_4 + 2H_2O$
   RWGS: $2CO_2 + 2H_2 \rightarrow 2CO + 2H_2O$
   Electrolysis: $4H_2O \rightarrow 4H_2 + 2O_2$
   Net: $3CO_2 + 2H_2 \rightarrow CH_4 + 2O_2 + 2CO$ (discarded)

Sabatier reactors operate at temperatures of 200-550 °C and pressures of 1-100 bar (Götz et al., 2016). Heat produced in the reaction must be removed. Higher pressures are more favorable, allowing higher conversion efficiency and production of high-grade heat that may be useful for other system elements. Several approaches, including fixed-bed, fluidized-bed, three-phase, and structured reactors have been explored. Many Sabatier devices (e.g., El Sherif and Knox, 2005; Murdoch et al., 2005; Junaedi et al., 2012, 2014; Kappmaier et al., 2016) are only designed to convert CO_2 to O_2, such as for air revitalization in the International Space Station and other spacecraft, and the CH_4 produced is typically discarded. These Sabatier devices should be contrasted with reactive CO_2 "scrubbing" devices intended for short-duration missions (e.g., James and Macatangay, 2009).

According to Junaedi et al. (2012), "Nickel is the traditional Sabatier catalyst that has been extensively investigated, while ruthenium was reported as the most active catalyst with the highest selectivity toward CH_4." Thompson (2015) reports that low-cost nickel (Ni), cobalt (Co), iron (Fe), and molybdenum (Mo) catalysts can be used in the Sabatier reactor, "although these metals generally require higher temperatures to achieve reasonable kinetics." Much more expensive catalysts include ruthenium (Ru), palladium (Pd), rhodium (Rh) and platinum (Pt) that can operate at lower temperatures. For space applications, performance rather than cost is of prime consideration (A. Meier, pers. commun., 2017), designs typically incorporate these more expensive catalysts.

Catalyst deactivation is a significant concern for some Sabatier reactor designs, with the microchannel device of Brooks et al. (2005) experiencing deactivation after only a few hundred hours (A. Meier, pers. commun., 2017). By comparison, negligible deactivation must occur after ~12,000 hours to fulfill the requirements of propellant production over 480 days as specified for the Mars Ascent Vehicle in NASA's Design Reference Architecture 5.0 (DRA 5.0) (Kleinhenz and Paz, 2017).

A propellant production designed for space applications using a microchannel Sabatier reactor has much lower mass (~10 kg) compared with the water electrolyzer (~50 kg) (Brooks et al., 2005). This system was sized for a robotic sample-return mission requiring 16% of the DRA 5.0 propellant mass. A larger device, sized for DRA 5.0 (7.0 t CH_4 and 22.7 t O_2 over 480 days), requires 200 kg for the water electrolyzer, but an unreported (e.g., negligible) mass for the Sabatier reactor (Kleinhenz and Paz, 2017). The microchannel Sabatier device also required a RWGS reactor, whose mass at half-scale for a robotic mission (~8% of DRA 5.0) was reported to be 0.5 kg (Holladay et al., 2007); thus a full-scale RWGS reactor for DRA 5.0 would be ~6.0 kg, much smaller than either the Sabatier reactor or electrolyzer.

As an exothermic reaction, the Sabatier reactor consumes essentially no energy, whereas the water electrolyzer in Kleinhenz and Paz consumes 24 kW (Kleinhenz and Paz, 2017). The RWGS reactor, being endothermic, does require some thermal energy; Muscatello and Santiago-Maldonado (2012) reported that thermally coupling it with a Sabatier reactor reduces net heat generated by 37%, a clever way to recycle excess heat.

We estimate that the mass of the Opus 12 EC stack at 124 kg, significantly smaller than the water electrolyzer specified in Kleinhenz and Paz. The additional mass (aside from radiator panels, which the Sabatier device would presumably require also) is only 20 kg. Together with the 36 kg CO_2-to-plastics device mass, the overall mass footprint is well below that of the Sabatier-based water electrolyzer system, yet the Opus 12 device offers significant versatility, namely the ability to produce multiple gases including C_2H_4 that can be converted into HDPE. Even if the EC stack were as massive as the water electrolyzer, the advantages of the Opus 12 are still strongly apparent.

6. CO_2-to-propellant sensitivity analyses

We have explored the sensitivity of the system mass to several key parameters shown in Table 5. As expected, higher EC efficiency and/or CH_4 share lowers scaled system mass. Moreover, raising the device operating temperature can result in a substantial reduction in system mass.

Table 5. Sensitivity analysis

Variable	**Value**	**System mass**	**Radiator panel area**	**Total pressure drop**	**Pipe inner diameter**	**Scaled system mass***
		kg	*m^2*	*bar*	*m*	*kg*
EC efficiency (% electrical energy in products)	50%	676.91	40.96	0.573	0.0180	950.79
	55%	631.55	37.44	0.433	0.0180	806.44
	60%	586.00	33.88	0.317	0.0180	685.92
	65%	540.65	30.34	0.224	0.0180	584.15
	70%**	412.19	26.86	0.509	0.0147	413.55
	75%	377.62	23.28	0.319	0.0147	353.60
	80%	343.19	19.71	0.181	0.0147	301.28
	85%	306.33	16.16	0.401	0.0112	253.10
CH_4 share (% energy	30%	411.73	26.85	0.509	0.0147	688.47

of total products) (sum of CH_4 + C_2H_4 is constant at 80%)	40% 50%** 60% 70%	411.91 412.19 412.27 412.45	26.85 26.86 26.85 26.85	0.509 0.509 0.509 0.509	0.0147 0.0147 0.0147 0.0147	516.58 413.55 344.69 295.58
Device operating temperature (K)	293 303 313** 323 333	512.06 456.94 412.19 376.94 347.23	36.95 31.38 26.86 23.29 20.29	0.701 0.595 0.509 0.442 0.385	0.0147 0.0147 0.0147 0.0147 0.0147	513.74 458.44 413.55 378.19 348.37
Mars surface temperature (K)	175 200 224** 250 275	389.89 398.87 412.19 435.87 473.73	24.60 25.51 26.86 29.25 33.07	0.467 0.484 0.509 0.555 0.627	0.0147 0.0147 0.0147 0.0147 0.0147	391.17 400.18 413.55 437.30 475.29
Mars sky temperature (K)	100 125 153** 175 200	405.30 407.43 412.19 418.24 429.47	26.16 26.37 26.86 27.47 28.60	0.496 0.500 0.509 0.521 0.543	0.0147 0.0147 0.0147 0.0147 0.0147	406.63 408.77 413.55 419.62 430.88
Pipe schedule (schedule number and wall thickness in cm)	5, 0.12** 10, 0.17 40, 0.28 80, 0.37	412.19 581.92 698.86 854.76	26.86 26.80 26.80 26.86	0.509 0.193 0.284 0.536	0.0147 0.0171 0.0158 0.0139	413.55 583.83 701.16 857.57
Pipe inner diameter (cm)	0.85 1.12 1.47** 1.80 2.34 3.01	376.33 413.35 412.19 495.39 501.04 505.70	29.40 27.17 26.86 26.79 26.79 26.79	14.685 2.393 0.509 0.150 0.035 0.008	0.0085 0.0112 0.0147 0.0180 0.0234 0.0301	377.56 414.71 413.55 497.02 502.69 507.37

* Relative to CH_4 target production rate of 14.6 kg/day. ** Base case.

We also explored the effect of changing the average surface and sky temperatures on Mars, since these are dependent on location as well as season. Note that the freezing points of CH_4 and C_2H_4 lie below the lowest Mars surface temperature explored in these sensitivity runs, but not below the lowest Mars sky temperature. While we assume that all parts of the device would be maintained at or above 40 °C (the operating temperature of the EC cell), detailed thermal modeling will be required to ensure that no component is exposed to cold ambient temperatures to the degree that they would adversely affect device performance.

Changing the Mars surface temperature by ±50 K had a larger effect than changing the sky temperature by a similar amount. Because the average Mars sky temperature in the base case is ~75 K lower than the surface temperature, radiator panel absorption of infrared radiation from the sky is much lower than from the Martian surface, resulting in a lower sensitivity when this parameter is varied.

In two other sets of sensitivity runs, the pipe inner diameter was varied along with the EC efficiency sensitivity runs while keeping the total pressure drop at a reasonable level (<1 bar). In other sensitivity runs, the pipe diameter was kept fixed, except for the two sensitivities that explicitly explored its variation. The effect of increasing the pipe schedule (which increases pipe thickness) along with a simultaneous variation in pipe diameter to maintain acceptable pressure drop simply served to increase system mass. Changing just the pipe inner diameter while keeping pipe schedule fixed changed system mass and pressure drop in opposite directions. For the two smallest pipe diameters, the pressure drop was unacceptably high (>1 bar).

7. CO_2-to-plastics reactor

The input gas mixture is compressed to ~24 bar, with the majority sent to fill a buffer tank that is periodically injected into the fluidized bed reactor every ~150 s. A portion of this flow (~10% or ~1.5 mmol/s) is injected into a prepolymerization stage, along with catalyst (~20 μmol/s) and 97% CH_4 (~200 μmol/s) that acts as a carrier gas for the catalyst. The prepolymerization stage is important to maintain a consistent molecular mass of product, though a range of molecular masses is inevitable and can actually enhance polymer mechanical properties. A very small amount of catalyst (0.005-0.5 mol% of polymer product according to Mun, 2002; Evertz et al., 1992 reported <0.0001 mol%) is needed to produce small polymer "seed" particles. To increase the accessible surface area, the prepolymer can be treated with *n*-hexane to remove low molecular weight polymer, but given the challenges of providing additional reagents on Mars, we assume this step is skipped at the expense of lower porosity and subsequently greater catalyst mass needed; here we assume the upper end (0.5 mol%) in our model. The recommended temperature is between 40 °C and 115 °C; we assume 80 °C in our model. Reagents are heated with a small resistive heat element prior to entry into the prepolymer reactor.

When the buffer tank has reached full capacity of 0.57 mol C_2H_4 (total gas mixture is 2.08 mol) after 152 s, the cycling valve is opened, emptying the contents of the buffer tank into the fluidized bed reactor. If the reactor is starting from cold conditions, the gas mixture is heated to ~90 °C before entering the reactor; however, the reaction itself is exothermic, producing heat in excess of what is needed to maintain the reaction conditions, so the heating element is not needed under normal operational conditions. Prepolymer product is meanwhile being continuously fed into the fluidized bed reactor to attain full-sized polymer chains with additional C_2H_4 and ~70 μmol of hydrogen (H_2) gas fed through the bottom of the reactor. H_2 must be included as a co-reagent to control polymer molecular mass: with an average chain length for HDPE of ~7,000 to ~100,000 C_2H_4 units (Reusch, 2013), and one H_2 molecule needed per HDPE molecule to terminate the chain, the H_2/C_2H_4 ratio is ~0.001% to ~0.014%; we assume the upper end of this range in our model. Note that because H_2 reacts much less frequently with the catalyst than C_2H_4, the concentration of H_2 in the reactor is ~5 mol% (Fernandes and Lona, 2000) despite its much lower flow rate.

There are a number of catalyst choices available for making HDPE. For gas-phase reaction, the Phillips catalyst (chromium(II) bis(cyclopentadienyl) oxide or variants) supported on silica/alumina is preferred. Other alternatives are Ziegler-Natta catalysts, which have many variations but are generally $TiCl_4$ supported on $MgCl_2$, with triethyl (or other trialkyl) aluminum

co-catalyst added separately to the reactor feed. However, Ziegler-Natta catalysts are generally used in liquid solvent systems. For the reactor design specified here, we assume a pure chromium-based Phillips catalyst, though Mun (2002) indicates that triethylaluminum is also used in the pre-polymer stage of their design. Clearly, due to the complexity of these catalysts, they must be brought from Earth, but fortunately, only very small amounts are required: a five-year supply for a system producing 9.2 kg/day of HDPE with 90% uptime requires only 140 kg.

As mentioned above, unlike the continuous flow design described in Mun (2002), we opt for a batch mode design in order to achieve the secondary objective of high CH_4 purity in the product gas stream. Because CH_4 does not participate in the polymerization reaction, it is enriched with each pass of the mixture through the reactor, as C_2H_4 is converted into solid polymer. By allowing the reaction to proceed without injecting more C_2H_4/CH_4 mixture into it, the C_2H_4 (and very small amount of H_2) is progressively depleted, leaving almost pure CH_4. In continuous flow designs, the reactor gas flow rate is ~2-8 times the minimum flow required for fluidization (Fernandes and Lona, 2000; Mun, 2002) and ~50 times (1.70 mol/s) that of the reagent input rate. We assume a similar flow rate in our batch design, and estimate that the per-pass conversion rate is 2% of the amount of C_2H_4 remaining in the gas stream. Therefore, as C_2H_4 is depleted, the reaction rate slows. We calculate that 114 passes are required to achieve 90% C_2H_4 conversion. At this point, the total pressure has dropped to 18 bar due to consumed C_2H_4.

The reactor dimensions are estimated based on ratios suggested in Mun (2002) to be 7.4 cm in diameter and 61 cm long, for a total internal volume of 2,612 cm^3. Assuming 24 bar initial pressure and 90 °C operating temperature (see below), the gas mixture will contain 0.57 mol C_2H_4, 1.51 mol CH_4, trace amounts of other gases, as well as the 0.07 mol of solid prepolymer. (It may also contain a ~few mol% of CO_2 depending on the upstream separation process, but the presence of CO_2 will not have any effect on the reaction and so can be considered part of the inert fraction with CH_4.) The total gas mixture is 2.08 mol initially. Moreover, the prepolymerization reactor consumes an additional 0.23 mol of gas, for a total of 2.31 mol. Therefore, at the Opus 12 reactor output rate of 4.15 mmol/s C_2H_4, it requires 152 s to refill the reactor. However, rather than taking this entire period to refill the reactor after each batch, we assume that the reactor is purged and refilled quickly from a buffer tank, which then slowly fills again over the next period. We assume that it takes ~14 s to accomplish this cycling, leaving 139 s left to run the batch reaction itself. With 115 required passes, each pass takes 1.219 s, which is consistent with the calculated cycle rate of the reactor.

The temperature of fluidized bed reactor must operate between 70 and 115 °C; we choose 90 °C in our model. Both the prepolymerization and fluidized bed reactor stages generate considerable heat (396 W in total) liberated as a byproduct of polymerization, which is more than sufficient to heat the incoming gases to the desired working temperatures. The heat remaining as well as waste heat from other processes (gas compression, cyclonic separation—see below) is dissipated in the heat exchanger after the reactor.

The unreacted gas mixture exits the top of the fluidized bed reactor where it passes through a cyclone, a type of centrifuge designed to remove any fine polymer particles suspended in the gas stream. Solid particles fall to the bottom of the cyclone, where they are combined with the bulk of the polymer solids coming out of the reactor.

While it is more efficient to send the gas flow through the heat exchanger before the compressor, newer designs have switched the order to reduce fouling of the cooler by fine polymer particles. However, such designs still require periodic servicing, which is not a realistic option for our design because it is not expected that astronauts will be present to perform maintenance; the plant must run for several years without a shutdown. Therefore, we have included a secondary high efficiency particulate air (HEPA) filtration stage after the cyclone in order to remove all remaining particle fines and eliminate the need for maintenance. HEPA filters are designed to remove >99.97% of particles ≥0.3 μm in diameter, and they perform even better than that at smaller particle sizes (Wikipedia, 2018). It is not expected that the HEPA filter will need frequent replacement, but it could be easily replaced by an astronaut or even, conceivably, a robotic system.

After the batch cycle concludes, a second cycling valve opens to purge the resulting mixture from the reactor tank (adding the small amounts of solid particles recovered from the cyclone) and passing it through a degasser (basically a solid/gaseous separator) to produce the HDPE and enriched CH_4 products. The production rates are 9.2 kg/d of HDPE and 11.3 mmol/s of gas mixture (97% CH_4, 3% C_2H_4). Small amounts of this enriched CH_4 mixture are used as an inert buffer gas for entraining the powdered catalyst during injection into the prepolymer phase, as described above. We assume 200 μmol/s of 97% CH_4 is used.

Note that the polymer production rate is more than twice the maximum requirement (2-4 kg/d). This is because we assumed a scaled-up reactor sufficient to provide 15.2 kg/d CH_4, slightly higher than the 14.6 kg/d required by the NASA DRA 5.0 Mars Ascent Vehicle (7.0 t over 480 d). If the device is not also required to produce propellant, it can be scaled down significantly.

The overall heat rejection budget for the polymerization system is summarized in Table 3.

Table 6. Heat budget of CO_2-to-plastics system

Item	**Heat load (W)**
Initial gas compression from 1 to 24 bars	238
Dissipated by first heat exchanger	–238
Pre-polymerization stage:	
• Heat liberated during reaction	43
• Heat absorbed in raising temperature of C_2H_4/CH_4 mixture	–4
Fluidized bed reactor stage:	
• Heat liberated during polymerization	352
• Heat absorbed in raising temperature of C_2H_4/CH_4 mixture	–35
Main cyclone	132
Gas recompression from 18 to 24 bars	26
Dissipated by second heat exchanger	–514
Degasser cyclone	1
Total heat generated by CO_2-to-plastics reactor	**754**

Fernandes and Lona (2000) claim that a sufficiently high gas flow rate in the fluidized bed reactor will prevent polymer melting and hence build-up of solid material on reactor walls. However, according to Mun (2002), large chunks of polymer can be still be formed within the fluidized bed reactor, potentially blocking the recycle gas flow or even the entire polymerization zone, unless the reactor is shut down and the sheets are removed. Although our design mostly avoids buildup of polymer fines that could coat the inside surfaces of critical equipment (such as valves, heat exchanger or compressor), periodic human maintenance may still be necessary, though it is yet unclear how frequently such maintenance may be required.

Acknowledgments

I would like to thank the following people for contributing to the final version of this report: Dr. John Hogan (NASA Ames Research Center), Dr. Anne Meier (NASA Kennedy Space Center), Dr. Tim Merkel (MTR, Inc.) and Dr. Daniel Miller (Lawrence Berkeley National Laboratory). I also gratefully acknowledge Dr. Etosha Cave (Opus 12, Inc.) for selecting Emerging Futures for this project, and for working closely with me throughout the 18-month duration, as well as NASA for providing funding through contract number NNX17CJ02C.

References

Brooks, K.P., Rassat, S.D., and TeGrotenhuis, W.E., 2005. Development of a Microchannel In Situ Propellant Production System, Final Report, Pacific Northwest National Laboratory, U.S. Department of Energy Grant No.: DE-AC05-76RL01830, September.

Callaghan, C., 2006. Kinetics and catalysis of the water-gas-shift reaction, Ph.D. thesis. http://www.che.utah.edu/~ring/DesignII/Articles/Water%20Gas%20Shift%20Kinetics-c%20callaghan%20thesis.pdf.

El Sherif, Dina and James C. Knox, 2005. International Space Station Carbon Dioxide Removal Assembly (ISS CDRA) Concepts and Advancements, 2005-01-2892. https://ntrs.nasa.gov/archive/nasa/casi.ntrs.nasa.gov/20050210002.pdf.

Engineering Toolbox, no date. Bursting and Collapsing Pressures of ASTM A312 Stainless Steel Pipes. https://www.engineeringtoolbox.com/stainless-steel-pipes-bursting-pressures-d_463.html. Accessed 6 September 2018.

Evertz, Kaspar, Roland Saive, Guido Funk, Peter Koelle, Rainer Konrad, Hans Gropper, 1992. Phillips catalyst and its use for the preparation of ethylene homopolymers and copolymers, U.S. patent number US5352658A, 13 February. https://patents.google.com/patent/US5352658.

Fernandes, F. A. N., L. M. F. Lona, 2000. Fluidized bed reactor for polyethylene production. The influence of polyethylene prepolymerization, *Braz. J. Chem. Eng.* 17 (2), DOI: 10.1590/S0104-66322000000200004. http://ref.scielo.org/n6pzs6.

Götz, M. J. Lefebvre, F. Mörs, A. M. Koch, F. Graf, et al., 2016. Renewable Power-to-Gas: A technological and economic review, *Renewable Energy* 85: 1371-1390.

Holladay, J.D., K.P. Brooks, R. Wegeng, J. Hu, J. Sanders, S. Baird, 2007. Microreactor development for Martian in situ propellant production, *Catalysis Today* 120 (2007) 35–44.

Hoskins, David, 2017. How to Remove Moisture From Natural Gas, *Sciencing*, 25 April. https://sciencing.com/remove-moisture-natural-gas-8756813.html. Accessed 14 September 2018.

James, John T. and Ariel Macatangay, 2009. Carbon Dioxide – Our Common "Enemy." https://ntrs.nasa.gov/archive/nasa/casi.ntrs.nasa.gov/20090029352.pdf.

Junaedi, Christian, Kyle Hawley, Dennis Walsh and Subir Roychoudhury, Morgan B. Abney and Jay L. Perry, 2012. Compact and Lightweight Sabatier Reactor for Carbon Dioxide Reduction, 42nd International Conference on Environmental Systems, International Conference on Environmental Systems (ICES), American Institute of Aeronautics and Astronautics, AIAA 2012-3482, 15-19 July, San Diego, CA. https://arc.aiaa.org/doi/abs/10.2514/6.2012-3482.

Junaedi, Christian, Kyle Hawley, Dennis Walsh and Subir Roychoudhury, Morgan B. Abney and Jay L. Perry, 2014. CO_2 Reduction Assembly Prototype using Microlith-based Sabatier Reactor for Ground Demonstration. 44th International Conference on Environmental Systems ICES-2014-090 13-17 July 2014, Tucson, AZ.

Kappmaier, Fabian, Carsten Matthias, Johannes Witt, 2016. Carbon Dioxide Reprocessing Subsystem for Loop Closure as part of the Regenerative Life Support System ACLS, 2016. 46th International Conference on Environmental Systems ICES-2016-391, 10-14 July 2016, Vienna, Austria.

Kleinhenz, Julie E., Aaron Paz, 2017. An ISRU Propellant Production System to Fully Fuel a Mars Ascent Vehicle, American Institute of Aeronautics and Astronautics, AIAA SciTech Forum, 9-13 January, Grapevine, TX, Paper number 20170001421. https://ntrs.nasa.gov/search.jsp?R=20170001421.

Lima, D. F. B., et al., 2012. Modeling and Simulation of Water Gas Shift Reactor: An Industrial Case. (full ref at end of doc). http://cdn.intechopen.com/pdfs/34193/InTech-Modeling_and_simulation_of_water_gas_shift_reactor_an_industrial_case.pdf.

Ma, Haotian, Li lan, Liu Yi Fei, Luo Yu, Shan Yu, 2009. Water Gas Shift Reactor Design, Presentation for CN2116 Group 28, AY0809 Semester 2, Published on 28 September. https://www.slideshare.net/l16cn/water-gas-shift-reactor-design.

Morrison, Chris, 2018. The Pylon: Near-Term Commercial LEU Nuclear Fission Power for Mars and the Moon, *Mars Society 2018 Convention*, Pasadena, CA, 25 August 2018.

Mun, Tham Chee, 2002. Production of Polyethylene Using Gas Fluidized Bed Reactor, National University of Singapore. https://pdfs.semanticscholar.org/eaa8/47ce6cbad3a55f6e6fa7d9e9307181d1b54b.pdf or

http://www.klmtechgroup.com/PDF/Articles/articles/Fluidized-Bed-Reactor.pdf. Accessed 2 May 2018.

Murdoch, Karen, Joel Goldblatt, Robyn Carrasquillo and Danny Harris, 2005. Sabatier Methanation Reactor for Space Exploration, 1st Space Exploration Conference: Continuing the Voyage of Discovery AIAA 2005-2706 30 January - 1 February 2005, Orlando, Florida.

Muscatello, A., E. Santiago-Maldonado, 2012. Mars In Situ Resource Utilization Technology Evaluation, NASA Kennedy Space Center, Cape Canaveral, FL; AIAA-2012-360, 50th AIAA Aerospace Sciences Meeting, Nashville, Tennessee, Jan. 9-12. https://ntrs.nasa.gov/search.jsp?R=20160005057.

Reusch, W., 2013. Polymers. Last updated 5 May. https://www2.chemistry.msu.edu/faculty/reusch/virttxtjml/polymers.htm. Accessed 30 May 2018.

Sigma-Aldrich. (2017). Molecular Sieves - Technical Information Bulletin. http://www.sigmaaldrich.com/chemistry/chemical-synthesis/learning-center/technical-bulletins/al-1430/molecular-sieves.html. Accessed 14 September 2018.

Thorlabs, 2018. HT24S - 24 W, 20 mm x 20 mm Metal Ceramic Heater. https://www.thorlabs.com/thorproduct.cfm?partnumber=HT24S and https://www.thorlabs.com/_sd.cfm?fileName=CTN002042-S01.pdf&partNumber=HT24S (specification sheet). Accessed 22 September 2018.

TubeWeb, no date. Non-Ferrous Tube: Theoretical Bursting & Collapsing Pressures For Pipe Stainless Steel (ASTM-A-312). http://www.tubeweb.com/Non-Ferrous-Tube/theoretical-bursting-collapsing-pressures-for-pipes.html. Accessed 23 December 2017.

Wikipedia, 2017. Water-gas shift reaction. Last updated 20 November. https://en.wikipedia.org/wiki/Water-gas_shift_reaction.

Wikipedia, 2018. HEPA. Last edited 3 May 2018. https://en.m.wikipedia.org/wiki/HEPA. Accessed 7 May 2018.

Additional references can be found in the six quarterly reports as well as the spreadsheet models that are being made available as part of the final deliverable for this project.

